

# Robust R-peak Detection using Deep Learning based on Integrating Domain Knowledge

Oleksii Kovalchuk<sup>a</sup>, Pavlo Radiuk<sup>a</sup>, Olexander Barmak<sup>a</sup>, Iurii Krak<sup>b,c</sup>

<sup>a</sup> Khmelnytskyi National University, 11, Institutes str., Khmelnytskyi, 29016, Ukraine

<sup>b</sup> Taras Shevchenko National University of Kyiv, 64/13, Volodymyrska str., Kyiv, 01601, Ukraine

<sup>c</sup> Glushkov Cybernetics Institute, 40, Glushkov ave., Kyiv, 03187, Ukraine

## Abstract

Electrocardiography (ECG) is a pivotal clinical technique for assessing heart function by recording its electrical activity. However, accurate processing and analysis of ECG signals, particularly the detection of R-peaks, remains challenging. Any inaccuracies in R-peak detection can significantly impact subsequent stages of analysis, potentially leading to incorrect diagnoses and treatment decisions. Therefore, in this study, we aim to refine the approach to identifying R-peaks in ECG signals by integrating knowledge of a reference ECG signal into the input signal, addressing the critical need for accurate R-peak detection in diagnosing various cardiac pathologies. The authors propose a novel method involving the integration of knowledge into the ECG signal, processing this information using a convolutional neural network, and post-processing the CNN model's results to identify R-peaks. The method was evaluated using various four well-known ECG databases. Comparative results, with an error margin of  $\pm 25$  ms, revealed that the proposed approach was the top performer across almost all metrics and databases, frequently achieving accuracy scores of 0.9999 and demonstrating high precision, recall, and  $F_1$ -score. Based on the investigation findings, the proposed approach is robust and reliable, with the best performance achieved on the QT database test set, offering a balanced and dependable solution for R-peak detection in ECG signals.

## Keywords <sup>1</sup>

Healthcare diagnosis, electrocardiogram, ECG monitoring, R-peak detection, domain knowledge, deep learning

## 1. Introduction

The exploration of Electrocardiogram (ECG) processing through artificial intelligence (AI) and deep learning (DL) paradigms has opened up avenues for more precise and timely cardiac anomaly detection, significantly impacting patient care and outcomes. A pivotal component of ECG analysis is the detection of R-peaks, which are crucial for determining heart rate and other cardiac parameters [1], [2]. The accurate detection of these peaks is integral for diagnosing a myriad of cardiovascular diseases [3].

A standard ECG comprises 12 leads, obtained using 10 electrodes [4]. This allows for the measurement of the heart's overall electrical potential from 12 different angles. A typical ECG signal diagram is presented in Fig. 1.

---

IDDM'2023: 6th International Conference on Informatics & Data-Driven Medicine, November 17–19, 2023, Bratislava, Slovakia  
EMAIL: losha.kovalchuk1998@gmail.com (O. Kovalchuk); radiukpavlo@gmail.com (P. Radiuk); alexander.barmak@gmail.com (O. Barmak); yuri.krak@gmail.com (I. Krak)  
ORCID: 0000-0001-9828-0941 (O. Kovalchuk); 0000-0003-3609-112X (P. Radiuk); 0000-0003-0739-9678 (O. Barmak); 0000-0002-8043-0785 (I. Krak)



© 2023 Copyright for this paper by its authors.  
Use permitted under Creative Commons License Attribution 4.0 International (CC BY 4.0).  
CEUR Workshop Proceedings (CEUR-WS.org)

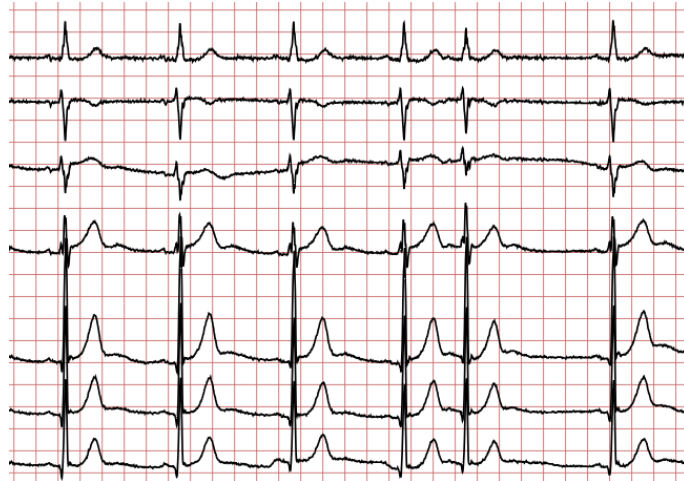


**Figure 1:** Schematic illustration of leads12 of an ECG signal [4].

The application of DL in ECG processing presents some challenges that are reflective of the broader issues in the fusion of healthcare and emerging technologies. Any issues in R-peak detection can adversely affect all subsequent stages of processing, analysis, and classification of the ECG-signal. Accordingly, high accuracy in recognizing R-peaks is crucial for advancing the field and unlocking the full potential of AI and DL in cardiac care. Thus, the primary contribution of this research is the refinement of the approach to identifying R-peaks in the ECG signal by integrating knowledge of a reference ECG signal into the input signal.

The structure of the paper is as follows. In Section 2, we review existing methods for R-peak detection in ECG signals. Section 3 is comprehensive, detailing the novel approach for R-peak detection, the CNN architecture used, post-processing methods, datasets employed, neural network training, and evaluation criteria. In Section 4, the paper examines the results obtained, where we compare our approach with existing analogs and discuss the implications of the results. Finally, Section 5 concludes the study findings and discusses the potential for future research.

## 2. Related works

The primary method of preparing ECG signals for use in DL models involves segmenting cardiac cycles based on the R-peaks present in the signal. R-peak detection influences the quality of applying DL methods to address core tasks such as classification and identification [5]. Thus, providing high accuracy in recognizing R-peaks is mandatory for prompt and robust cardiac care.

One of the primary hurdles is the diversity and complexity of ECG data. The morphology of ECG signals can vary extensively among individuals due to factors such as age, gender, and underlying cardiac or systemic conditions. This heterogeneity necessitates the development of robust algorithms capable of accurately identifying R-peaks amidst a plethora of signal forms [6]. DL models, especially convolutional neural networks (CNNs), have shown promise in handling such complex data, yet their performance can be significantly influenced by the quality and amount of data they are trained on.

Moreover, the issue of data quality and accessibility is another significant challenge. High-quality, labeled ECG data is essential for training reliable DL models [7]. However, obtaining such data is often encumbered by privacy concerns, as well as logistical and financial hurdles [8]. Additionally, the labeling of ECG data requires expertise in cardiology, further constraining the availability of high-quality training data.

Furthermore, the interpretability of DL models remains a major concern. The “black-box” nature of these models can lead to resistance from healthcare professionals who might find it difficult to trust or understand the decisions made by the AI [9]. This lack of transparency also poses challenges in identifying and correcting errors in R-peaks detection, which is critical for ensuring patient safety and effective diagnosis.

Currently, there are numerous methods and approaches to detecting the R-peak in ECG signals, with their effectiveness often reported as approximately 99%. However, in such studies, a large margin of error

is typically used, or it is not mentioned at all. For instance, in study [10], a high reported result for peak detection in the ECG signal was achieved, but the margin of error was as high as  $\pm 75$  milliseconds. This value results in an overall error window of 150 milliseconds, which exceeds the length of the entire QRS complex under normal conditions.

Porr et al. [11] conducted a meta-analysis in their article regarding the results of approaches such as: Pan and Tompkins by Fariha et al. [12], Hamilton and Tompkins by Ahmad et al. [13], Christov by Xiong et al [14], and Kalidas by Ivora et al. [15]. As a result of this study, the authors found that each article reported very high accuracy rates of 98% or more. This can likely be attributed to large time tolerances, possibly 100 milliseconds or even more.

Another prominent toolbox for ECG processing is NeuroKit2 [16]. It is an open-source Python tool tailored for efficient neurophysiological signal processing, catering to both beginners and experts. Its comprehensive suite for varied signals, from ECG to EMG, ensures broad applicability in research scenarios. NeuroKit2's advantages are broad signal compatibility, user-centered design, and emphasis on research transparency, as for disadvantages, – potential learning curve for novices and reliance on community contributions for updates and improvements.

Therefore, in this study, we aim to develop a novel approach based on CNN to R-peak detection in ECG signals, focusing on reducing the permissible error during peak determination.

### 3. Methods and materials

To enhance existing approaches for detecting R-peaks in ECG signals, a method illustrated in Fig. 2 has been proposed.

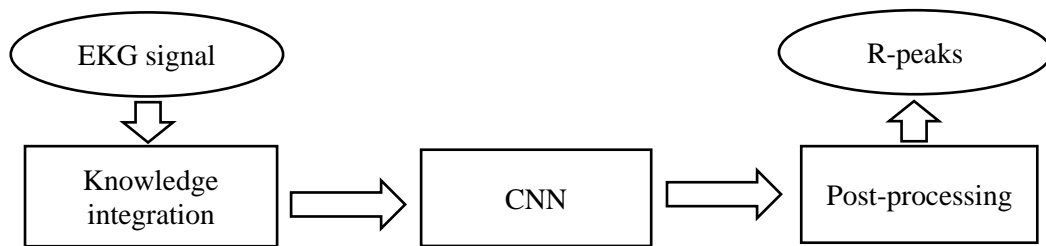


**Figure 2:** Schematic of the traditional approach to R-peak detection.

In this approach, it is suggested to integrate knowledge about the reference cardiac cycle into the input ECG signal. Specifically, the following stages of information transformation are proposed:

1. Integration of knowledge about the ECG signal.
2. Processing of information using a CNN model.
3. Processing the results of the CNN model to identify R-peaks.

#### 3.1. Integration of knowledge into the ECG signal

It is known that in the I-II and V1-V6 leads of the ECG signal, a distinctive feature of the R-peak is the most positive deviation of the signal at a certain part of the signal. To integrate this knowledge into each segment of the ECG signal from the formed samples, the steps outlined in Fig. 3 are applied.

The input receives an ECG signal,  $S$ , in the form of a one-dimensional array of values. Based on the length of the signal, the  $K$  array is initialized with zero values, into which integrated knowledge is recorded.

In **step 1** of the algorithm, a segment of 260 elements is taken from the ECG signal. This number of elements was determined experimentally and is sufficient to cover a cardiac cycle.

In **step 2**, a theoretical identification of the R-peak is conducted, specifically the maximum positive deviation,  $p$ , in the obtained signal segment. The identified maximum deviation undergoes verification to determine if it is the peak of a wave. If the deviation doesn't increase from the left and decrease from the right, then the found deviation is not at the wave's peak, and the process returns to the first step to process the next part of the signal. If the verification is successful, the process moves to the next step.

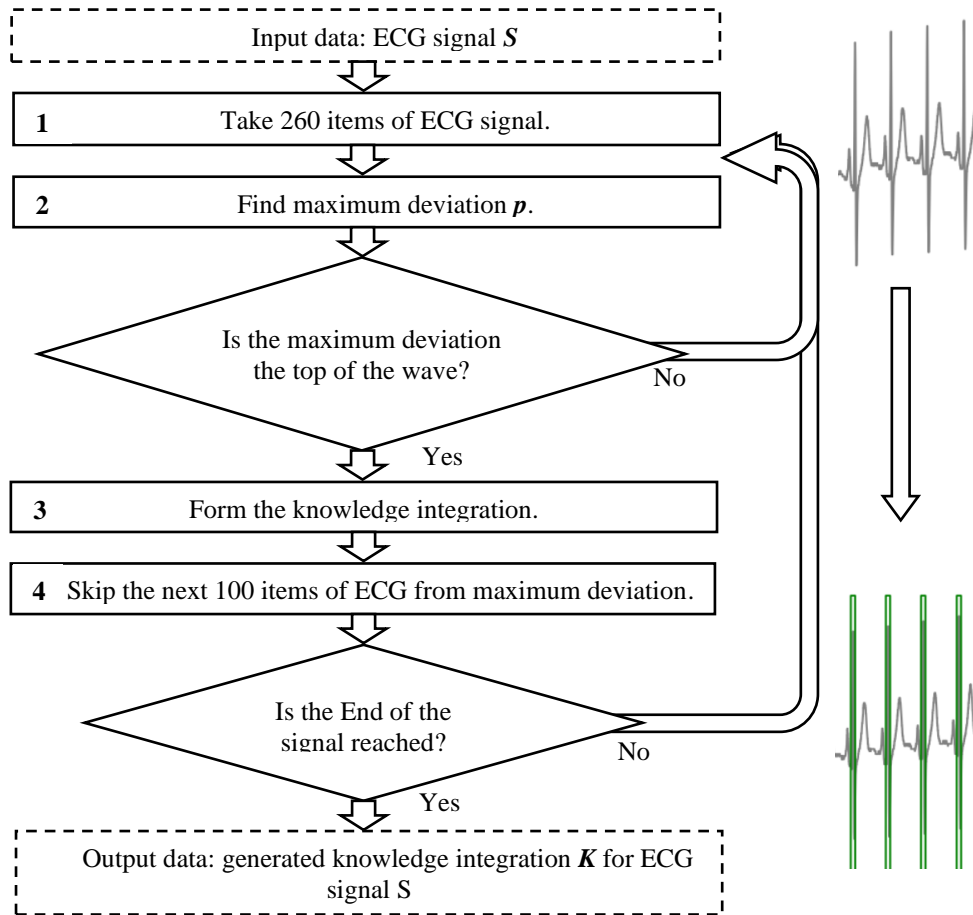


**Figure 3:** Scheme of the proposed approach to the extraction of R-peaks.

**Step 3** involves populating the  $K$  array with knowledge. Based on the identified peak, its global index,  $i$ , in the ECG signal  $S$  is determined. Subsequently, the  $K$  array is filled with a value of 1 in the range  $[i-20, i+20]$ . This range typically covers the QRS complex, which includes the R-peak.

**Step 4** is optimization oriented. It aims to avoid searching for a new maximum deviation (theoretical R-peak) immediately after the deviation  $p$  found in step 2, as R-peaks appear at specific intervals.

The outcome of the algorithm is the populated  $K$  array. The visualization of overlaying knowledge on the ECG signal is shown in Fig. 4.

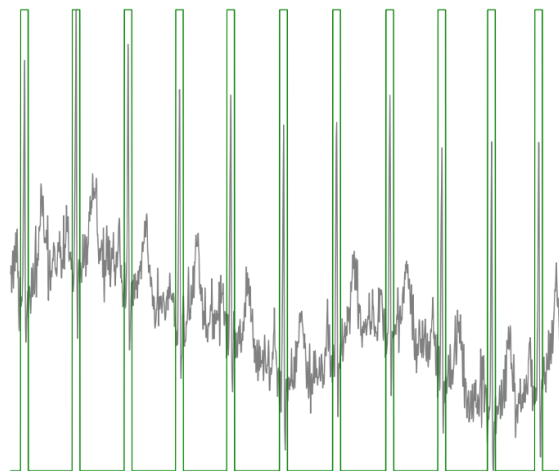


**Figure 4:** The result of the integration of knowledge into the ECG signal according to the proposed approach.

### 3.2. CNN architecture for detecting R-peak

At this stage, based on the results of existing approaches to the determination of R-peaks by neural network means, it is proposed to use the following neural network architecture (Table 1).

**Table 1**

Architecture of the utilized CNN.

Layer name	Input	Output	kernel_size	stride	padding	Scale factor
<i>Encoder</i>						
Conv1d	2	32	3	1	1	
ReLU						
MaxPool1d			2	2		
Conv1d	32	64	3	1	1	
ReLU						
MaxPool1d			2	2		
Conv1d	64	128	3	1	1	
ReLU						
MaxPool1d			2	2		
Conv1d	128	256	3	1	1	
ReLU						
MaxPool1d			2	2		
<i>Decoder</i>						
Upsample						2
Conv1d	256	128	3	1	1	
ReLU						
Upsample						2
Conv1d	128	64	3	1	1	
ReLU						
Upsample						2
Conv1d	64	32	3	1	1	
ReLU						
Upsample						2
Conv1d	32	1	3	1	1	
ReLU						
Sigmoid						

### 3.3. Post processing to determine R-peaks

The final stage is designed to process the output of the CNN model, P, to convert it into indices where the R-peaks are located in the input signal. The output from the CNN network is an array of the same dimension as the input array with the ECG signal. An example of the CNN network's output is illustrated by the red line in Fig. 5.

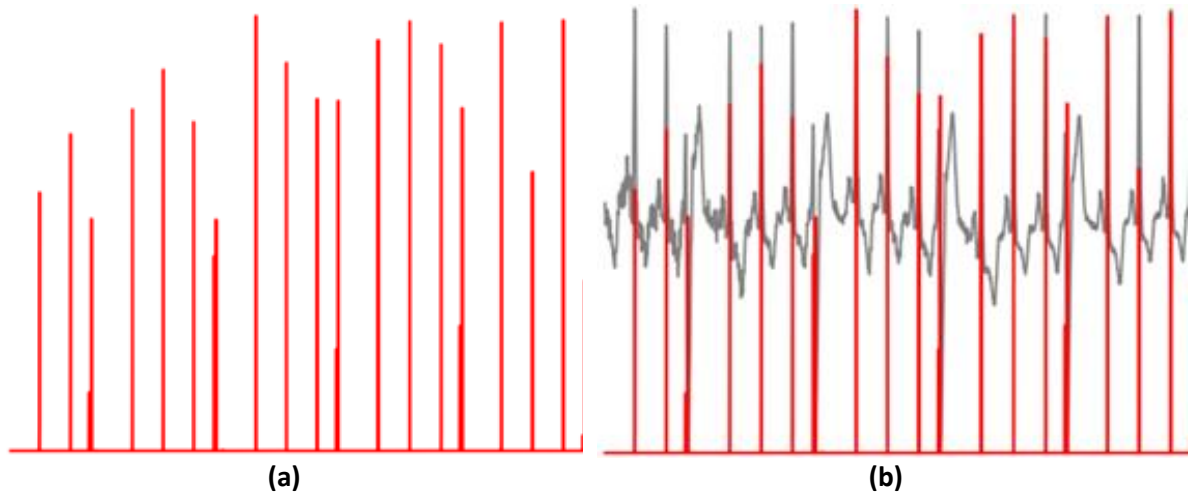


**Figure 5:** Output of the CNN: (a) the initial output from the CNN, (b) the overlaid initial output of the CNN on the input ECG signal.

The indices of the R-peaks correspond to the indices of the P array elements where the values exceed a specified threshold. In our study, this threshold is set at 0.1. Additionally, indices are merged if there is a short interval between the identified segments of indices.

### 3.4. Datasets

In this work, the following four datasets with ECG signals were used:

- MIT-BIH Arrhythmia Database (MIT-BIH) [17].
- QT Database (QT) [18].
- China Physiological Signal Challenge-2020 Database (CPSC-2020) [19].
- University of Glasgow Database (UoG) [20].

**MIT-BIH Arrhythmia Database.** From the MIT-BIH dataset, signals numbered 108 and 207 were excluded because parts of the annotation in these signals do not correspond to the peak apex, thereby preventing accurate training and testing of the neural network. An example of such a signal is shown in Fig. 6.

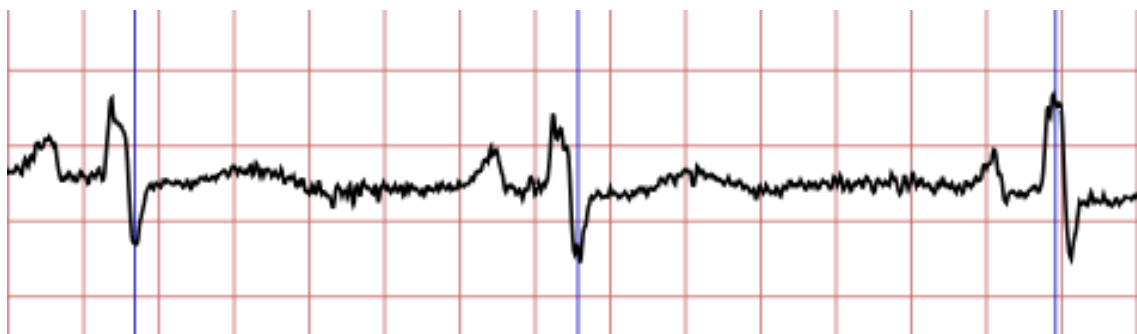


**Figure 6:** An example of a labeled ECG signal from MIT-BIH [17].

**QT Database.** Signals belonging to QT have been filtered. From this dataset, signals containing an incomplete (non-standard) ECG signal were removed. An example of such a signal is presented in Fig. 7.

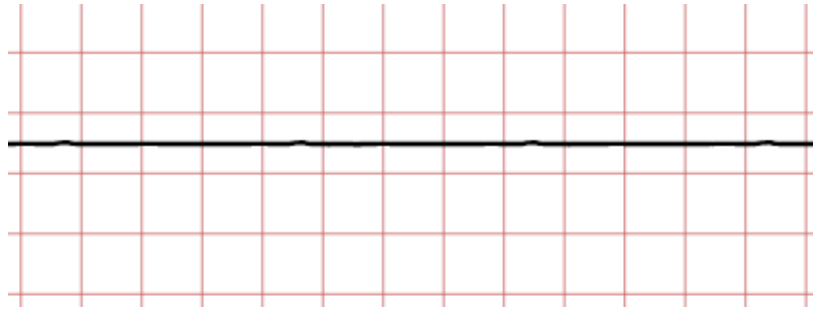


**Figure 7:** An example of an incorrect ECG signal from MIT-BIH that was extracted from [17].

Given that the signals in the mentioned databases have varying frequencies, additional transformations were carried out to ensure that all signals from all databases had a frequency of 400 Hz. Signals from these datasets were segmented into fragments of length 4000 for their subsequent use as input signals for the neural network. Fragments obtained from datasets 1-3 were divided into training and testing sets in a 70/30 ratio, respectively.

**High Precision ECG Database – University of Glasgow.** From this dataset, a separate independent test set of signals was created. The test set included signal fragments recorded from lead II during the following experiments (activities): sitting, maths, and walking. Table 2 presents the number of fragments included in the training and testing sets.

**Table 2**

Distribution of signals in the used data set.

Sample title	Database title	The number of signal fragments
Training data	MIT-BIH	68811
	MIT-BIH	2484
Test data	QT	2148
	CPSC 2020	24861
Unique test data	ECG Database – UoG	876

### 3.5. Training of a neural network

For training the network, 70% of the dataset formed from the MIT-BIH, QT, and CPSC-2020 databases was used. The training was conducted in two stages. The loss curves for the training and validation datasets are shown in Fig. 8.

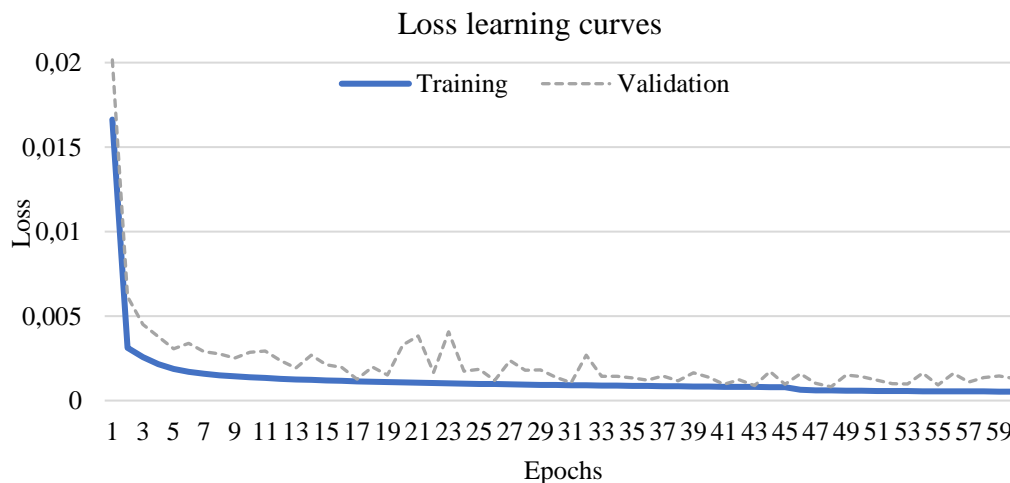


**Figure 8:** Training and validation loss learning curves.

During the first stage of training, the Adam optimizer was used for 45 epochs with a learning rate of 0.001. In this stage, a loss value of 0.000821 was achieved. In the second stage, training was conducted over 15 epochs with a learning rate of 0.0001, resulting in a loss value of 0.000580. The total training time was 82 minutes.

### 3.6. Evaluation criteria and experiment setup

Let us represent the count of positive and negative instances in the initial dataset by P and N, respectively. Applying a classifier categorizes objects into true positives (TP), true negatives (TN), false positives (FP), and false negatives (FN). This research evaluated the suggested method using various statistical measures as outlined below.

$$\text{Accuracy} = \frac{\text{TP} + \text{TN}}{\text{TP} + \text{TN} + \text{FP} + \text{FN}} \quad (1)$$

$$\text{Precision} = \frac{\text{TP}}{\text{TP} + \text{FP}} \quad (2)$$

$$\text{Recall} = \frac{\text{TP}}{\text{TP} + \text{FN}} \quad (3)$$

$$F_1 = \frac{2\text{TP}}{2\text{TP} + \text{FP} + \text{FN}} \quad (4)$$

In training our network, we employed the Adam optimizer across 10 epochs, meticulously setting the training parameters based on insights and empirical evidence from our previous research [21], [22]. Specifically, we manually selected a learning rate within the range of 0.0001 to 0.001, set the weight decay at 0.0005, fixed the momentum at 0.85, and chose a batch size of 64. This process took place on a single NVIDIA GeForce GTX 1650 GPU, spanning approximately 155 minutes.

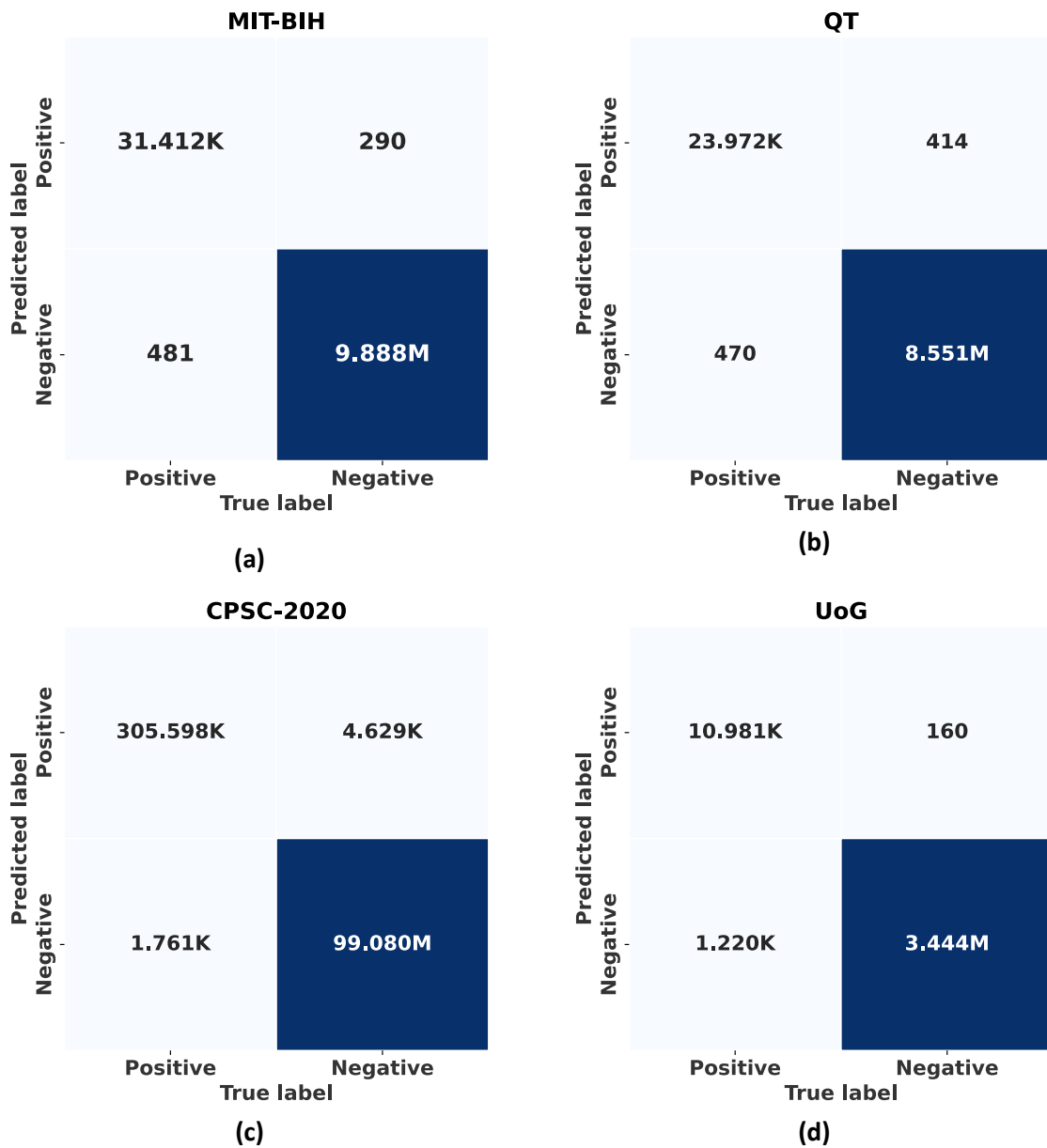
It is noteworthy that we opted for manual hyperparameter tuning over automatic optimization. This decision was grounded in our extensive experience in deep learning for R-peak detection, as detailed in our prior works. We recognized that the unique characteristics and challenges of R-peak detection render the task highly sensitive to hyperparameter choices. Given this sensitivity, and the fact that automatic hyperparameter optimization can sometimes lead to suboptimal and overfit models in such contexts, we concluded that a manual, knowledge-driven approach was more appropriate. This approach ensured that our model was not only tailored to the specificities of R-peak detection but also benefited from the proven effectiveness of parameter values validated in our previous successful applications of deep learning in related domains.

Experiments were conducted using the following software: Python 3.9 [23], Scikit-learn [24], and PyTorch [25]. The system utilized for these experiments had the following specifications: Intel Core i7 9th Gen, 16GB RAM, and an NVIDIA GeForce GTX 1650 GPU with 4 GB of video memory.

## 4. Results and discussion

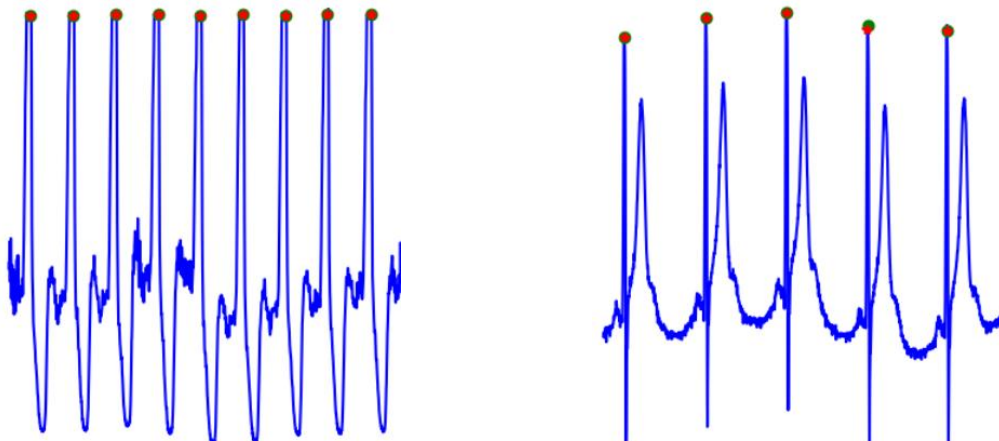
When calculating the presented metrics, an error margin of  $\pm 25$  ms (equivalent to  $\pm 10$  points) is used. Testing of the proposed approach was conducted using test datasets, which were formed from data not included in the training sets. As a result of the calculations, confusion matrices were generated for each dataset, as shown in Fig. 9.





**Figure 9:** Confusion matrices obtained using the proposed approach from experimental testing with various ECG signal datasets: (a) MIT-BIH, (b) QT, (c) CPSC-2020, and (d) UoG.

Fig. 10 illustrates the R-peak detection obtained by the proposed approach.



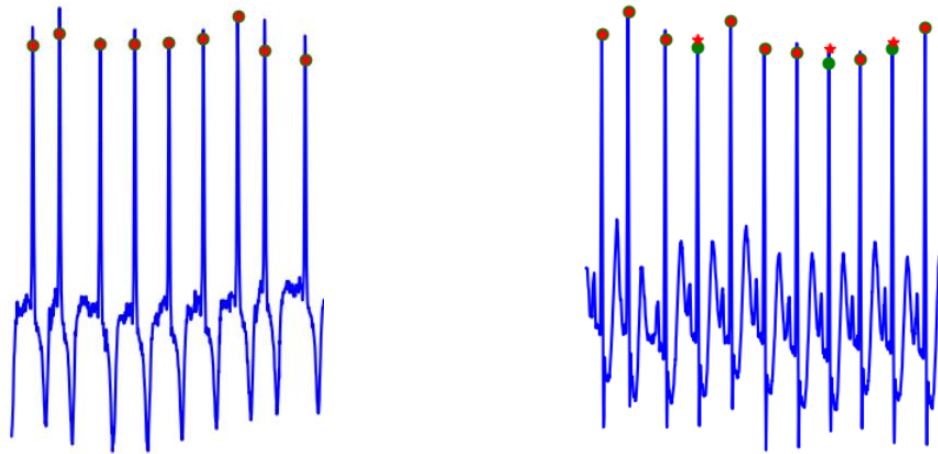


**Figure 10:** Visualizing different samples with detecting R-peaks obtained by the proposed approach. The red asterisk (\*) symbol denotes the R-peak according to the database annotation, and the green circle indicates the calculated position of the R-peak.

A thorough analysis was also conducted on cases where the statistical indicators were found to be lower. Fig. 11(a) illustrates a case where the proposed approach identified an R-peak that was not annotated in the database. The result shown in Fig. 11(b) depicts a case where the R-peaks annotated in the database are marked as a negative deviation, which in this instance is incorrect.

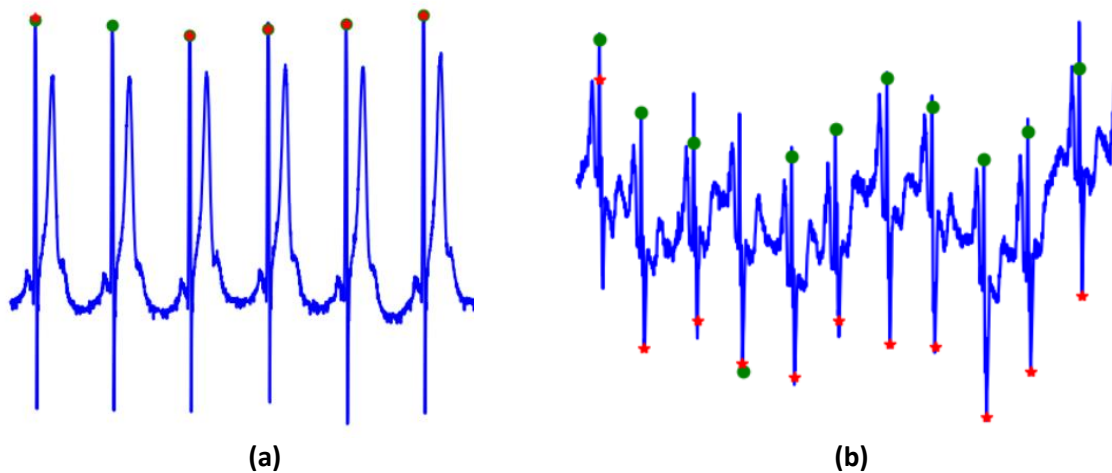


**Figure 11:** Analysis of cases for which the statistical indicators were lower: (a) an R-peak that was not annotated in the database, (b) a case where the R-peaks annotated in the database are marked as a negative deviation.

The results of R-peak detection using the proposed approach were compared with analogues: Rodrigues et al. [1], Koka et al. [6], Zahid et al. [10], and NeuroKit2 [16]. When calculating the statistical indicators, a proposed error margin of  $\pm 25$  ms was used. The comparative data presented in Table 3 for the five approaches across four test datasets – MIT, QT, CPSC-2020, and UoG – on metrics of Accuracy, Precision, Recall, and  $F_1$ -score, gives insight into their performance and efficacy in different contexts.

Analyzing accuracy from Table 3, it is apparent that the approaches by Zahid et al. and Ours are the standout performers across all databases, frequently achieving a score of 0.9999. They marginally outperform the others, demonstrating a higher level of detecting R-peaks. NeuroKit2 also demonstrates high accuracy but slightly trails behind Zahid et al. and Ours.

Precision is a metric that further emphasizes the robustness of Zahid et al. and Ours, especially in the MIT and CPSC-2020 databases, where their scores hover around 0.99 (Table 3). Such an outcome

suggests that these approaches have a high rate of true positive predictions. NeuroKit2 follows suit with commendable precision, notably in the UoG database, where it scores 0.9932, surpassing even Zahid et al. and Ours.

**Table 3**

Results of the R-peaks detection. Reminder: ECG signals from the UoG database were not included in the training set.

Database	Approach	Accuracy	Precision	Recall	F <sub>1</sub> -score
MIT	NeuroKit2	0.9997	0.9644	0.9340	0.9490
MIT	Rodrigues et al.	0.9992	0.8322	0.9491	0.8868
MIT	Koka et al.	0.9992	0.8938	0.8699	0.8817
MIT	Zahid et al.	<b>0.9999</b>	0.9905	<b>0.9858</b>	<b>0.9881</b>
MIT	Our	<b>0.9999</b>	<b>0.9909</b>	0.9849	0.9879
QT	NeuroKit2	0.9997	0.9655	0.9410	0.9531
QT	Rodrigues et al.	0.9991	0.7824	0.9427	0.8551
QT	Koka et al.	0.9993	0.8866	0.8767	0.8816
QT	Zahid et al.	<b>0.9999</b>	0.9789	0.9778	0.9783
QT	Our	<b>0.9999</b>	<b>0.9830</b>	<b>0.9808</b>	<b>0.9819</b>
CPSC-2020	NeuroKit2	0.9997	0.9514	0.9514	0.9514
CPSC-2020	Rodrigues et al.	0.9989	0.7763	0.9212	0.8426
CPSC-2020	Koka et al.	0.9995	0.9232	0.8972	0.9100
CPSC-2020	Zahid et al.	<b>0.9999</b>	<b>0.9855</b>	0.9927	0.9891
CPSC-2020	Our	<b>0.9999</b>	0.9851	<b>0.9943</b>	<b>0.9897</b>
UoG	NeuroKit2	<b>0.9998</b>	<b>0.9932</b>	0.9596	<b>0.9761</b>
UoG	Rodrigues et al.	0.9996	0.9083	<b>0.9990</b>	0.9515
UoG	Koka et al.	0.9994	0.9194	0.8968	0.9080
UoG	Zahid et al.	0.9995	0.9838	0.8666	0.9215
UoG	Our	0.9996	0.9856	0.9000	0.9409

For recall, different databases reflect varying levels of recall for the five approaches (Table 3). Rodrigues et al. exceeds others in the UoG database with a near-perfect recall of 0.9990, although its precision is lower. Zahid et al. maintains strong recall performance in the CPSC-2020 database with a score of 0.9927, indicating a high sensitivity to detecting true positives.

The F<sub>1</sub>-score, which is the harmonic mean of precision and recall, reveals a balanced performance for Zahid et al. and Ours across all databases. They consistently achieve high F<sub>1</sub>-scores, indicating a balanced ratio of precision to recall. NeuroKit2 also shows a balanced performance, particularly in the UoG database with a value of 0.9761, hinting at its reliability.

In summation, the approaches by Zahid et al. and Ours are markedly the top performers across almost all metrics and databases, demonstrating a balanced and reliable performance. Their high scores in accuracy, precision, and F<sub>1</sub>-score depict them as robust and dependable approaches. Rodrigues et al. and NeuroKit2 exhibit specific strengths in recall and precision respectively in certain databases, but they do not match the all-rounded performance of Zahid et al. and Ours.

Visual analysis of the detection results showed that in certain segments of the ECG signal, our approach identifies more R-peaks. For instance, Fig. 12 illustrates a comparison of each method's performance on a similar ECG signal, where our proposed approach yielded more accurate results.

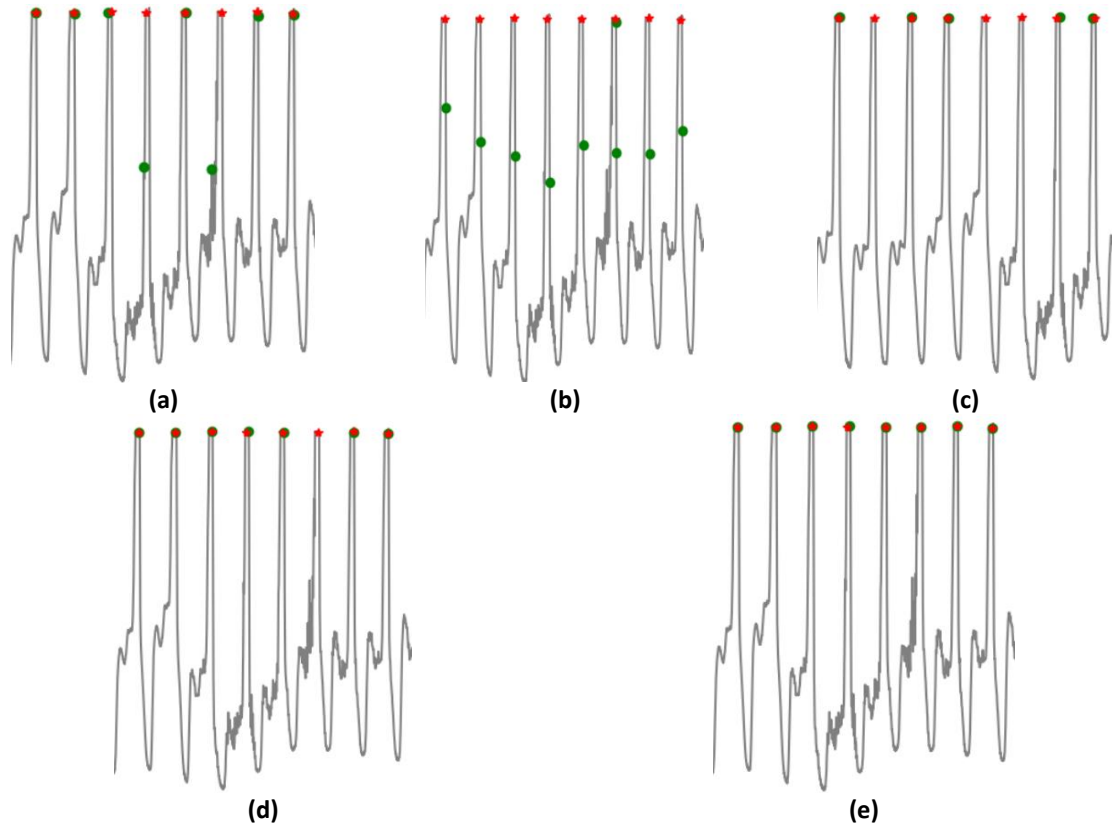


**Figure 12:** Visual comparison of the results of R-peak detection by the considered approaches: (a) NeuroKit2, (b) Rodrigues et al., (c) Koka et al., (d) Zahid et al, (e) Our approach. Red labels indicate the location of R-peaks annotated by medical experts, and green labels indicate the R-peaks identified by the respective approach.

As per Fig. 12, the observations are as follows:

- NeuroKit2 detected two R-peaks with incorrect positioning.
- Rodrigues et al. located almost all R-peaks with some positional errors.
- Koka et al. missed three R-peaks.
- Zahid et al. failed to detect 1 peak.
- The proposed approach accurately identified all R-peaks.

It should be also noted that the best performance of the proposed approach compared to analogues was achieved on the test set derived from the QT database. For an independent dataset based on the UoG database, our approach ranked second. This suggests that this dataset contains ECG signals with characteristics that are either absent or minimally present in the training set. As a result, the CNN model may not be fully equipped to recognize the R-peak for such ECG signals. For NeuroKit2, such characteristics are less critical, as it identifies R-peaks as local maxima in QRS complexes found by the steepness of the ECG signal's absolute gradient.

## 5. Conclusions and Future work

In this study, we focused on refining the approach to identifying R-peaks in the ECG signal by integrating knowledge of a reference ECG signal into the input signal. The significance of accurate R-peak detection is emphasized, as it forms the foundation for subsequent analyses of the ECG signal and the diagnosis of various cardiac pathologies.

To enhance existing R-peak detection techniques, a novel approach was proposed, which integrates knowledge about the reference cardiac cycle into the input ECG signal. The process involves three main stages: (i) the integration of knowledge about the ECG signal, (ii) the processing of this information using a CNN model, (iii) and post-processing of the results of the CNN model to identify R-peaks. The

CNN architecture utilized was detailed, encompassing both encoding and decoding layers, and was trained using datasets like MIT-BIH, QT, and CPSC-2020.

The evaluation of the proposed method was comprehensive using test samples of MIT-BIH, QT, CPSC-2020, and UoG. An error margin of  $\pm 25$  ms was used for calculating metrics. The results were compared with other approaches that represent the state of the art in ECG processing. The proposed method consistently demonstrated high performance across various metrics and databases. Specifically, in the MIH-BIH and QT databases, the proposed approach outperformed its analogs achieving 99.99%. A visual analysis further substantiated the efficacy of the proposed approach, showing that it often identified more R-peaks accurately compared to other methods.

However, the research acknowledged certain limitations. In some segments of the ECG signal, the proposed approach identified more R-peaks, which could be a point of contention. Additionally, while our approach performed exceptionally well in most cases, there were instances where it missed or inaccurately positioned R-peaks.

Future research could delve deeper into refining this integration, exploring other neural network architectures, applying a wider set of clinical knowledge for further integration, and expanding the application to other aspects of ECG analysis. The potential to further reduce the error margin and achieve even more precise results remains an exciting prospect.

## 6. References

- [1] R. Rodrigues and P. Couto, "Semi-supervised learning for ECG classification," in 2021 Computing in Cardiology (CinC), Brno, Czech Republic, 13-15 September 2021: IEEE, Sep. 2021, pp. 1–4. doi: 10.23919/CinC53138.2021.9662693.
- [2] P. M. Tripathi, A. Kumar, R. Komaragiri, and M. Kumar, "A review on computational methods for denoising and detecting ECG signals to detect cardiovascular diseases," *Arch Computat Methods Eng*, vol. 29, no. 3, pp. 1875–1914, May 2022, doi: 10.1007/s11831-021-09642-2.
- [3] T. Anbalagan, M. K. Nath, D. Vijayalakshmi, and A. Anbalagan, "Analysis of various techniques for ECG signal in healthcare, past, present, and future," *Biomedical Engineering Advances*, vol. 6, p. 100089, 2023, doi: 10.1016/j.bea.2023.100089.
- [4] "The ECG leads: Electrodes, limb leads, chest (precordial) leads and the 12-Lead ECG," *ECG & ECHO*. Accessed: Sep. 26, 2023. [Online]. Available: <https://ecgwaves.com/topic/ekg-ecg-leads-electrodes-systems-limb-chest-precordial/>
- [5] X. Peng, H. Zhu, X. Zhou, C. Pan, and Z. Ke, "ECG signals segmentation using deep spatiotemporal feature fusion U-Net for QRS complexes and R-peak detection," *IEEE Transactions on Instrumentation and Measurement*, vol. 72, pp. 1–12, 2023, doi: 10.1109/TIM.2023.3241997.
- [6] T. Koka and M. Muma, "Fast and sample accurate R-peak detection for noisy ECG using visibility graphs," in 2022 44th Annual International Conference of the IEEE Engineering in Medicine & Biology Society (EMBC-2022), Glasgow, Scotland, United Kingdom, 11-15 July 2022: IEEE Inc., 2022, pp. 121–126. doi: 10.1109/EMBC48229.2022.9871266.
- [7] O. Kovalchuk, P. Radiuk, O. Barmak, and I. Krak, "A novel feature vector for ECG classification using deep learning," in Proceedings of the 4th International Workshop on Intelligent Information Technologies & Systems of Information Security (IntellITSIS-2023), Khmelnytskyi, Ukraine, March 22–24, 2023: CEUR-WS, 2023, pp. 227–238. [Online]. Available: <https://ceur-ws.org/Vol-3373/paper12.pdf>
- [8] A. Raza, K. P. Tran, L. Koehl, and S. Li, "Designing ECG monitoring healthcare system with federated transfer learning and explainable AI," *Knowledge-Based Systems*, vol. 236, p. 107763, 2022, doi: 10.1016/j.knosys.2021.107763.
- [9] P. Radiuk, O. Kovalchuk, V. Slobodzian, E. Manziuk, and I. Krak, "Human-in-the-loop approach based on MRI and ECG for healthcare diagnosis," in Proceedings of the 5th International Conference on Informatics & Data-Driven Medicine, Lyon, France, 18-20 November: CEUR-WS.org, 2022, pp. 9–20. [Online]. Available: <https://ceur-ws.org/Vol-3302/paper1.pdf>

- [10] M. U. Zahid et al., “Robust R-peak detection in low-quality holter ECGs using 1D convolutional neural network,” *IEEE Trans. Biomed. Eng.*, vol. 69, no. 1, pp. 119–128, 2022, doi: 10.1109/TBME.2021.3088218.
- [11] B. Porr and P. W. Macfarlane, “A new QRS detector stress test combining temporal jitter and accuracy (JA) reveals significant performance differences amongst popular detectors.” *bioRxiv*, p. 722397, Jul. 27, 2023. doi: 10.1101/722397.
- [12] M. A. Z. Fariha, R. Ikeura, S. Hayakawa, and S. Tsutsumi, “Analysis of pan-tompkins algorithm performance with noisy ECG signals,” *J. Phys.: Conf. Ser.*, vol. 1532, no. 1, p. 012022, 2020, doi: 10.1088/1742-6596/1532/1/012022.
- [13] I. Ahmad, “QRS detection for heart rate monitoring,” *International Journal of Electrical Engineering and Technology*, vol. 11, no. 4, pp. 360–367, 2020.
- [14] H. Xiong, M. Liang, and J. Liu, “A real-time QRS detection algorithm based on energy segmentation for exercise electrocardiogram,” *Circuits Syst Signal Process*, vol. 40, no. 10, pp. 4969–4985, 2021, doi: 10.1007/s00034-021-01702-z.
- [15] A. Ivora et al., “QRS detection and classification in Holter ECG data in one inference step,” *Sci Rep*, vol. 12, no. 1, Art. no. 1, 2022, doi: 10.1038/s41598-022-16517-4.
- [16] D. Makowski et al., “NeuroKit2: A Python toolbox for neurophysiological signal processing,” *Behav Res*, vol. 53, no. 4, pp. 1689–1696, 2021, doi: 10.3758/s13428-020-01516-y.
- [17] G. B. Moody and R. G. Mark, “MIT-BIH Arrhythmia Database.” *physionet.org*, PhysioNet, 2005. doi: 10.13026/C2F305.
- [18] P. Laguna, R. G. Mark, A. L. Goldberger, and G. B. Moody, “The QT Database.” *physionet.org*, PhysioNet, 1999. doi: 10.13026/C24K53.
- [19] Z. Cai et al., “An open-access long-term wearable ECG database for premature ventricular contractions and supraventricular premature beat detection,” *Journal of Medical Imaging and Health Informatics*, vol. 10, no. 11, pp. 2663–2667, 2020, doi: 10.1166/jmihi.2020.3289.
- [20] L. Howell and B. Porr, “High precision ECG Database with annotated R peaks, recorded and filmed under realistic conditions.” University of Glasgow, University of Glasgow, Luis Howell, 2018. doi: 10.5525/gla.researchdata.716.
- [21] I. Krak, O. Barmak, and P. Radiuk, “Detection of early pneumonia on individual CT scans with dilated convolutions,” in *Proceedings of the 2nd International Workshop on Intelligent Information Technologies & Systems of Information Security (IntelITSIS-2021)*, T. Hovorushchenko, O. Savenko, P. Popov, and S. Lysenko, Eds., Khmelnytskyi, Ukraine, March 24–26, 2021: CEUR-WS.org, 2021, pp. 214–227. Accessed: May 09, 2021. [Online]. Available: <http://ceur-ws.org/Vol-2853/>
- [22] P. Radiuk, O. Barmak, and I. Krak, “An approach to early diagnosis of pneumonia on individual radiographs based on the CNN information technology,” *The Open Bioinformatics Journal*, vol. 14, no. 1, pp. 92–105, Jun. 2021, doi: 10.2174/1875036202114010093.
- [23] “Python 3.9.0,” *Python.org*. Accessed: Sep. 26, 2023. [Online]. Available: <https://www.python.org/downloads/release/python-390/>
- [24] F. Pedregosa et al., “Scikit-learn: Machine learning in Python.” *arXiv*, Jun. 05, 2018. doi: 10.48550/arXiv.1201.0490.
- [25] A. Paszke et al., “PyTorch: An imperative style, high-performance deep learning library,” in *Advances in Neural Information Processing Systems*, H. Wallach, H. Larochelle, A. Beygelzimer, F. d\textquotesingle Alché-Buc, E. Fox, and R. Garnett, Eds., Vancouver, BC, Canada, December 8–14, 2019: Curran Associates, Inc., 2019, pp. 8024–8035. [Online]. Available: <https://dl.acm.org/doi/abs/10.5555/3454287.3455008>